DEVELOPMENT OF A SUPERCONDUCTING PROTON LINAC FOR ADS

Nobuo Ouchi, Nobuo Akaoka, Hiroyuki Asano, Etsuji Chishiro,
Yuya Namekawa, Hiroyuki Suzuki, Tomoaki Ueno
JAERI, Japan

Shuichi Noguchi, Eiji Kako, Norihito Ohuchi, Kenji Saito, Toshio Shishido, Kiyosumi Tsuchiya
KEK, Japan

Kouichi Ohkubo, Masanori Matsuoka, Katsuya Sennyu
MHI, Japan

Takashi Murai, Toshihiro Ohtani, Chihiro Tsukishima
MELCO, Japan

Abstract

ADS require a high-intensity proton accelerator of which energy and beam power are about 1 GeV and 20-30 MW, respectively. JAERI, KEK, MHI and MELCO have conducted a programme for the development of a superconducting proton linac for the ADS since 2002. This programme, which is based on the achievement of the J-PARC design work, consists of two parts, development of a 972-MHz cryomodule and system design of a superconducting proton linac in the energy range between 0.1 and 1.5 GeV. In the development work of the 972-MHz cryomodule, a prototype cryomodule which includes two nine-cell cavities of $\beta = 0.725$, will be developed and the goal is stable operation in the horizontal tests at the surface peak field at 30 MV/m. In the system design work, a preliminary beam dynamics design has been determined with the configuration of a cryomodule with two 972-MHz, nine-cell elliptical cavities, and a room-temperature focusing magnet. This paper provides the present status of the cryomodule development and the system design.

Introduction

JAERI proposes an ADS which consists of superconducting proton linac, spallation target of lead-bismuth eutectic and a subcritical core. In this proposal, the energy and beam power of the superconducting proton linac are 1.5 GeV and 20-30 MW, respectively. JAERI has conducted an R&D programme for the ADS since 2002 in collaboration with national laboratories, universities and companies. This programme includes R&D on a superconducting proton linac, lead-bismuth technology and subcritical core design and technology.

The R&D on the superconducting proton linac, which is based on the achievement of the J-PARC design work, consists of two parts, development of a 972-MHz cryomodule [1] and the system design of a superconducting proton linac in the energy range between 0.1 and 1.5 GeV.

In the development work for the 972-MHz cryomodule, which is conducted by JAERI, KEK and MHI, a prototype cryomodule is currently being assembled. The cryomodule includes two 972-MHz nine-cell cavities of $\beta = 0.725$. The goal of this work is stable operation in the horizontal tests at the surface peak field at 30 MV/m, which corresponds to an accelerating gradient of about 10 MV/m. The cavity development, which includes the vertical tests, is mainly being performed at KEK. The horizontal tests will be performed at JAERI, where a 972-MHz klystron, also utilised for the high-power tests of the power couplers, is in operation.

In the system design work, which is conducted by JAERI, KEK and MELCO, a preliminary beam dynamics design has been established with a configuration of a cryomodule with two 972-MHz, nine-cell elliptical cavities, and a room-temperature focusing magnet. The total number of cryomodules and their length are outlined in this work.

Cryomodule development

Cryomodule design

Figure 1 shows an overview of the cryomodule. Two 972-MHz nine-cell elliptical cavities are installed in the cryomodule, for which the operating temperature is designed to be 2 K. Each cavity is surrounded by a jacket-type liquid helium (LHe) vessel made of titanium. A box-shaped LHe reservoir tank, which is located above the cavities, connects both LHe jackets.

Figure 1. Overview of the prototype cryomodule

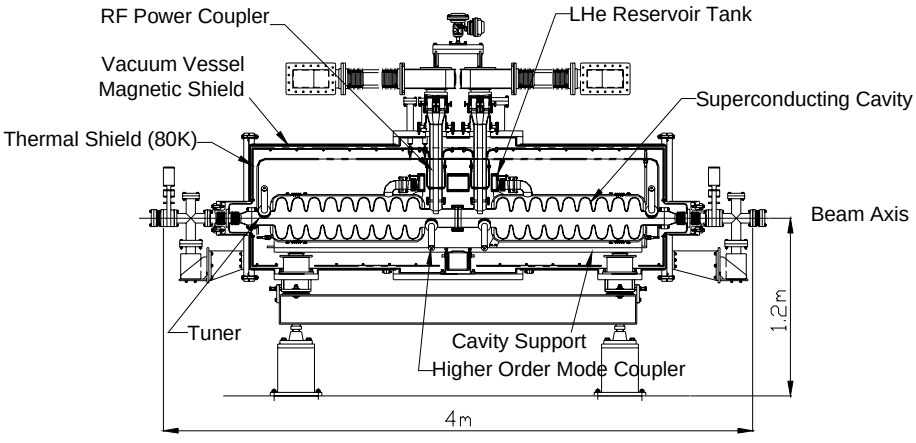

Coaxial-type power couplers, of which the inner and outer diameters are 34.7 mm and 80 mm, respectively, are located at the centre of the cryomodule. KEK-TRISTAN-type disk windows are placed at the room temperature region. Inner conductors of the power couplers and the windows are cooled by water. Cooling of the outer conductors is achieved by thermal intercepts at 5 K and 80 K. A high-power test of the power couplers was carried out successfully with a maximum RF power of 1 MW in pulsed mode operation; the pulse width and repetition rate are 0.6 ms and 25 Hz, respectively. Details of the power coupler design and the test results are presented in Ref. [2]. A higher-order mode (HOM) coupler is attached at both ends of each cavity. The HOM couplers located at the power coupler side are made of niobium and are designed to be cooled by LHe. The HOM couplers located at the outer side are made of copper without any cooling because of the reduced heating. Details of the design for the HOM coupler are presented in Ref. [1].

The tuning system consists of pulse motors and a piezo actuator is located outside the cryomodule. Each LHe jacket includes bellows and tuning force is applied from the tuning system with coaxial rods.

The heat shield at 80 K is installed in the cryomodule and is cooled by liquid nitrogen (LN_2). Thermal intercepts at both 80 K and 5 K, which are cooled by LN_2 and LHe, respectively, are also installed at power couplers, beam pipes and tuning rods. The cavity support is cooled by LN_2 at 80 K and the thermal insulation between the support and the cavity is achieved by GFRP. In order to achieve operation of the cavity at 2 K, a JT valve is installed in the cryomodule. Therefore, the cryomodule has three independent cryogenic flows, LN_2 at 80 K, LHe at 5 K and 2 K. The static heat load for each flow is estimated: 64 W, 16 W and 5 W for 80 K, 5 K and 2 K, respectively. A magnetic shield made of permalloy is installed just on the inner side of the vacuum vessel of the cryomodule.

Superconducting cavity

Figure 2 shows the shape of the 972-MHz, nine-cell cavity of $\beta = 0.725$, which includes the surrounding LHe jacket. The cell length and the total length including beam pipes are 112 mm and 1 397 mm, respectively. The equator and iris diameters are 277 mm and 90 mm, respectively, while the beam pipe diameter at the power coupler side is expanded to 126 mm in order to obtain sufficient external Q of the power coupler of $5 \cdot 10^5$. The RF parameters of this nine-cell cavity are summarised in Table 1 [3]. The wall thickness of this cavity is 3.8 mm, which is thicker than other superconducting elliptical cavities in order to provide the stiffness and to reduce the Lorentz force detuning. As the stiffness of the LHe jacket is also important to reduce the Lorentz force detuning, the shape of the end plates of the jacket was optimised so as to obtain sufficient stiffness. The stationary Lorentz force detuning was calculated to be 130 Hz at the surface peak field of 30 MV/m (i.e. accelerating field of about 10 MV/m).

Figure 2. 972-MHz, nine-cell elliptical cavity of $\beta = 0.725$

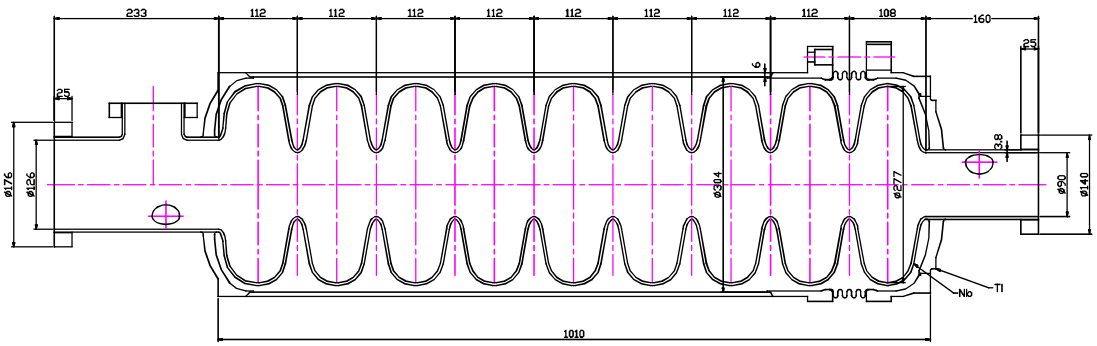

Table 1. RF parameters of the cavity

Esp/Eacc	3.07
Hsp/Eacc	55.4 Oe/(MV/m)
R/Q	478 Ω
Geometrical factor	208 Ω
Cell-to-cell coupling	2.80%

For the fabrication of the cavity, a new approach was applied in deep drawing; the shape of the die was optimised so as to minimise the forming error using a structural analysis and an error of less than 0.3 mm was obtained [4]. Pre-tuning was performed after fabrication of the cavity and field flatness above 98% was obtained for both cavities [5].Vertical tests of the cavities at 2 K were carried out after the surface treatments of barrel polishing and electropolishing. Figure 3 shows the final results of the vertical tests. Surface peak fields of 32 MV/m and 34 MV/m were obtained for two cavities (type-R and type-L cavities), which satisfied our target value of 30 MV/m.

Figure 3. Final results of the vertical tests of the cavities

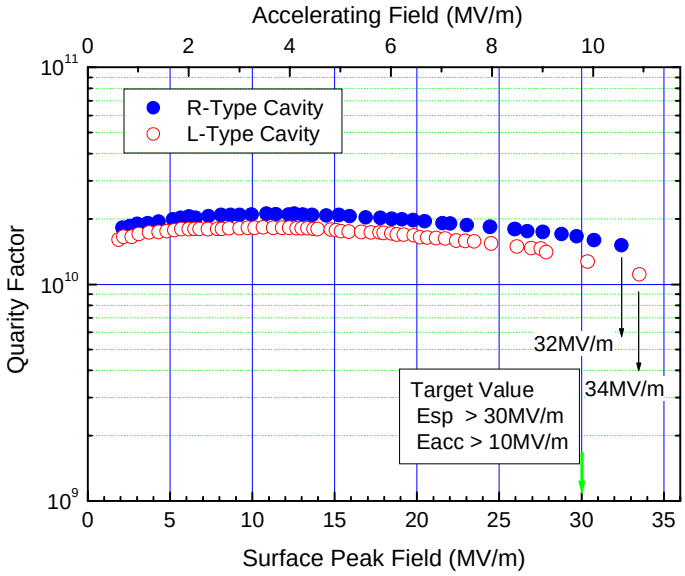

Cryogenic system for horizontal test

As described in the previous section, the cryomodule has three independent cooling lines of LN_2 at 80 K, LHe at 5 K and 2 K. Figure 4 shows a flow diagram of the cryogenic system for the horizontal test. The cryogenic system consists of the cryomodule, the valve box, the joint box, Dewars and other auxiliary components. Refrigerant for each line is fed from portable Dewar individually. The valve box is installed for connection and feed control of the refrigerants to the cryomodule. In the superconducting linac of the ADS plant, a similar valve box will be installed while the refrigerant will be fed directly from a refrigerator. The joint box is installed for the connection between the valve box and the Dewars, which is designed so as to exchange the Dewar during the experiment.

As for the line of LHe at 2 K, the LHe vessel is evacuated to about 4 kPa by a vacuum pump at the room temperature region. A vapour separator and a heat exchanger are equipped in the valve box in order to increase the production efficiency of LHe at 2 K in the cryomodule. The JT valve in the

Figure 4. Flow diagram of the cryogenic system for the horizontal test

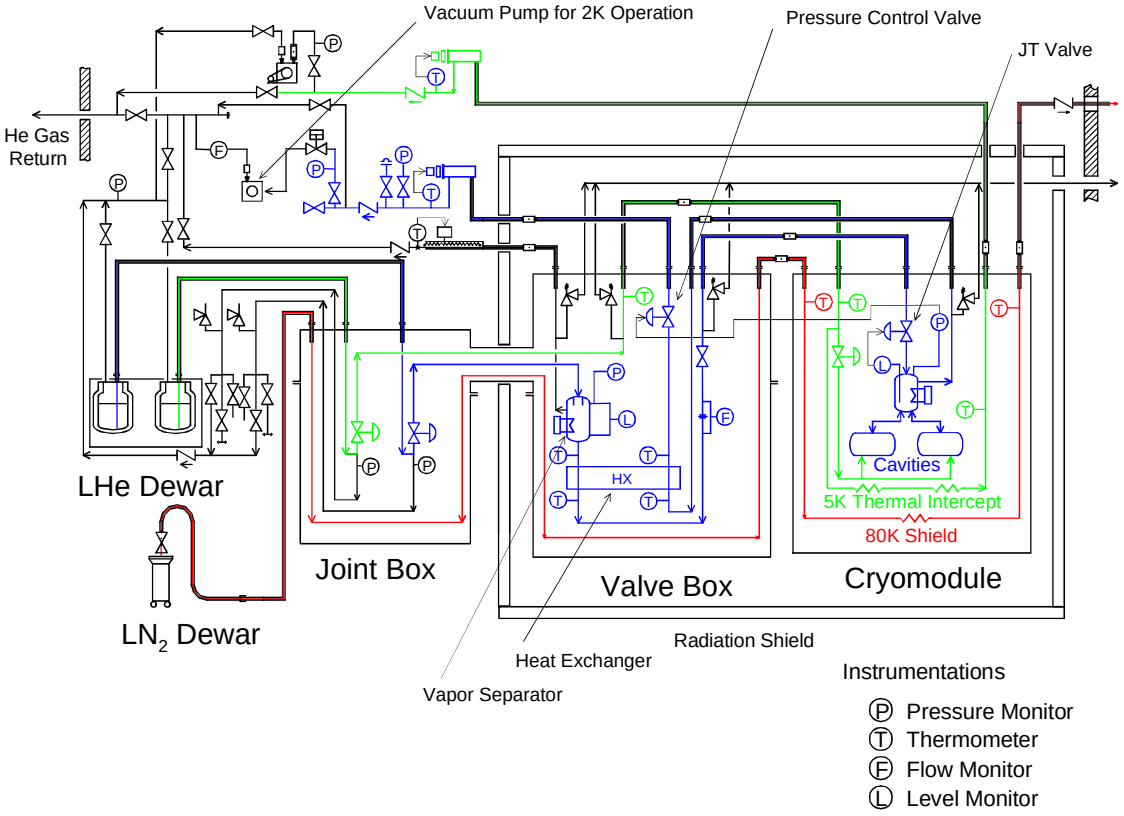

cryomodule produces the superfluid LHe and controls the LHe level in the LHe vessel. A valve placed on the He gas return line in the valve box performs pressure control of the LHe vessel, thus also temperature control of the LHe.

As for the line of LHe at 5 K, a valve in the joint box performs the flow control. In the cryomodule, this line is connected to the LHe vessel, which is used for the cooling down from room temperature to 5 K.

As for the line of LN_2, no control valve is placed in the cryomodule, the valve box and the joint box. The valve at the LN_2 Dewar performs the flow control manually.

Experimental arrangement and schedule of the horizontal test

The experimental arrangement of the horizontal test of the cryomodule is displayed in Figure 5. The cryomodule and the valve box are located in a radiation shield. The joint box, Dewars and the vacuum pump are located outside of the shield. An RF power source, klystron, is located at a lower level. A waveguide system is connected from the klystron and the RF power is divided for two cavities.

Final assemblage will be soon be complete at the JAERI Tokai site. The horizontal test is planned for 2004. In the test, the RF high power test will be performed for the final goal of the surface peak field of 30 MV/m. Additional testing planned includes cryogenic tests and low-level RF tests, including heat leak and temperature distribution measurement, a control test at 2 K operation, measurements of quality factors for the accelerating mode as well as HOMs, tuning tests and so on.

Figure 5. Experimental arrangement of the horizontal test

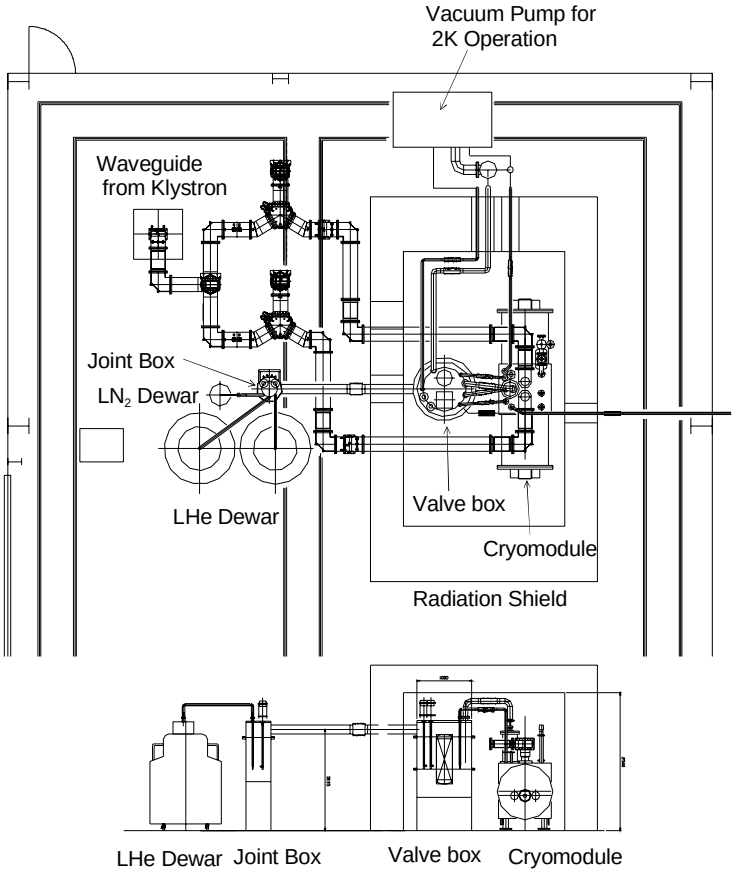

System design of superconducting linac for ADS

In the system design work, a preliminary beam dynamics design of the superconducting proton linac has been established in the energy range between 1 00 MeV to 1.5 GeV.

Basic design parameters

Table 2 shows the basic parameters for the beam dynamics design. In this energy range, the b value changes from 0.428 to 0.923. Parameters of accelerating frequency, number of cells in a cavity, number of cavities in a cryomodule and maximum surface peak field are set to be the same as the parameters of the prototype cryomodule. Phase slip in a cavity, which comes from a mismatch between beam b and cavity cell length, is set to be within −30 in order to obtain smooth bunching, as the synchronous phase angle is set to be -30 . According to this condition, the number of cavity groups is deduced to be 10 in the energy range 100 MeV to 1.5 GeV, which is larger than other superconducting linac designs because of the larger number of cells in a cavity of nine. The focusing magnet is considered to be a quadrupole doublet in a room temperature region between the adjacent cryomodules. The schematic view of the lattice structure is shown in Figure 6. The zero current transverse phase advance is set to be 70 , which is constant in a superconducting linac region. The longitudinal phase advance is obtained from the accelerating field of the cavity, while the maximum longitudinal phase advance is limited to 65 to avoid structural resonance in the beam dynamics.

Table 2. Basic parameters for the beam dynamics design

Energy range	100~1 500 MeV	Beam current	20~30 mA
b range	0.428~0.923	Synchronous phase	-30
Accelerating frequency	972 MHz	Phase slip in a cavity	Within −30
No. of cells in a cavity	9	No. of cavity groups	10
No. of cavities in a cryomodule	2	Focusing magnet	Room temperature
Max. surface peak field	<30 MV/m	Transverse phase advance	70 (I = 0A)

Figure 6. Schematic view of the lattice structure

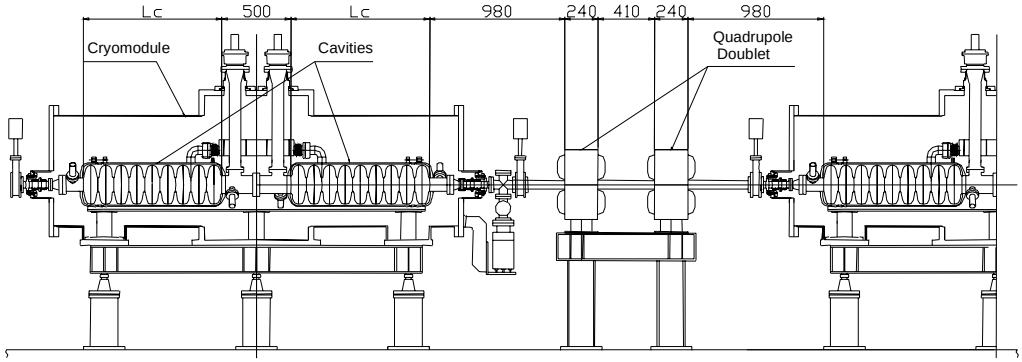

Preliminary superconducting cavity design

Preliminary designs of 10 kinds of superconducting cavities have been established in order to obtain the ratios of the surface peak field to the accelerating field and the transit time factors. Table 3 summarises the RF parameters of the cavities.

Table 3. RF parameters of the cavities

b	Esp/Eacc	Transit time factor	R/Q (W)
0.444	7.40	0.634	87.38
0.480	6.27	0.648	121.23
0.518	5.34	0.662	162.67
0.560	4.70	0.673	215.48
0.604	4.07	0.685	278.75
0.653	3.60	0.695	356.10
0.705	3.16	0.702	443.28
0.761	2.84	0.708	543.37
0.822	2.56	0.715	661.44
0.888	2.30	0.721	749.59

Lattice design

As shown in Figure 6, drift spaces between two cavities in the cryomodule, and between the cavity end and qadrupole magnet are set to be 500 mm and 980 mm, respectively. The effective length of the quadrupole magnet and drift space between the doublet are set to be 240 mm and 410 mm, respectively. These parameters are the same as for the superconducting linac design of the J-PARC project.

Table 4 summarises the structure of the superconducting linac. In this design, 106 cryomodules, i.e. 212 cavities, are necessary in the energy range from 100 to 1 500 MeV and total length is 560 m. As shown in Table 4, the lower-energy part, especially the 100-180 MeV region, is quite inefficient; 21 cryomodules and 100 m are necessary. The main reason for this inefficiency is a higher Esp/Eacc ratio. Optimisation of the lattice design as well as the cavity design is necessary for the final design of the superconducting linac.

Table 4. Basic structure of the superconducting linac

	Cavity b	Beam b	Beam energy (MeV)	No. of cryomodules	Length (m)
1	0.444	0.428~0.462	103.1~122.7	7	32.1
2	0.480	0.462~0.499	122.7~147.3	7	32.8
3	0.518	0.499~0.539	147.3~179.2	7	33.5
4	0.560	0.539~0.582	179.2~220.1	7	34.3
5	0.604	0.582~0.629	220.1~272.6	7	35.2
6	0.653	0.629~0.679	272.6~348.5	8	41.3
7	0.705	0.679~0.733	348.5~443.1	8	42.5
8	0.761	0.733~0.791	443.1~605.2	11	60.1
9	0.822	0.791~0.855	605.2~876.5	15	84.5
10	0.888	0.855~0.923	876.5~1 510	29	168.6
Total				**106**	**564.8**

Beam simulation

Beam simulation of the superconducting linac was performed using the TRACE-3D and modified PARMILA codes. In the simulation, the initial beam emittances are referred from the J-PARC beam design data. As an example of the results, Figure 7 shows the 90% emmittance in both transverse and longitudinal directions. As shown in the figure, emittance growth is not observed in the beam simulation results.

Figure 7. 90% emittance obtained in the beam simulation

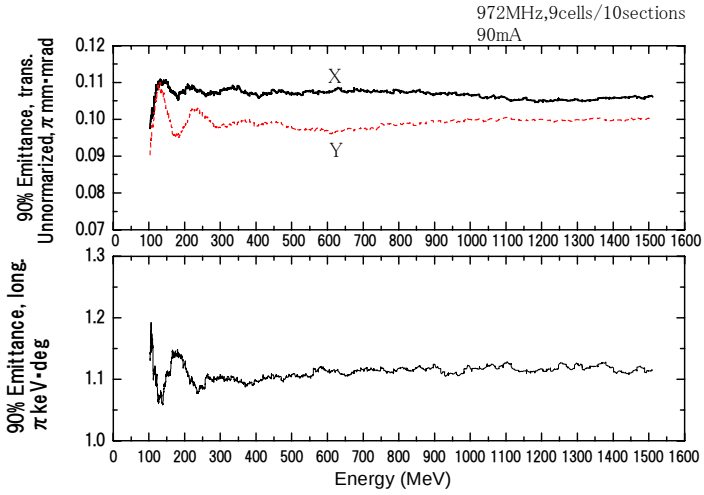

Conclusion

The development of a superconducting proton linac, cryomodule the system design are ongoing. As concerns the cryomodule, fabrication has been completed and final assemblage will soon be finished as well. The horizontal test will be performed in 2004 toward the goal of a maximum surface peak field above 30 MV/m. Regarding the system design, a preliminary beam dynamics design has been determined. The present result, however, provides more cryomodules and a longer total length than expected. Additional optimisation is thus necessary.

REFERENCES

[1] Noguchi, S., *et. al*., "Prototype Cryomodule for the ADS LINAC", *Proc. of the 11th Workshop on RF Superconductivity*, Luebeck/Travemuende, Germany (2003) MoP32, in press.

[2] Kako, E., S. Noguchi and T. Shishido, "Input Couplers for 972 MHz Superconducting Cavities in the High Intensity Proton Linac", *Proc. of the 11th Workshop on RF Superconductivity*, Luebeck/Travemuende, Germany (2003) ThP27, in press.

[3] Kako, E. and S. Noguchi, "RF Design of a 972 MHz Superconducting Cavity for High Intensity Proton Linac", *Proc. of EPAC2002*, Paris, France, pp. 2244.

[4] Saito, K., S. Noguchi and T. Ohta, "Half-cell Die Design for Right Cavity Geometry in High Intensity SC Proton Linac", *Proc. of the 11th Workshop on RF Superconductivity*, Luebeck/Travemuende, Germany (2003) TuP41, in press.

[5] Shishido, T., E. Kako and S. Noguchi, "Development of Pre-tuning System for 972 MHz 9-cell Superconducting Cavities", *Proc. of the 11th Workshop on RF Superconductivity*, Luebeck/ Travemuende, Germany (2003) TuP42, in press.

TABLE OF CONTENTS

Foreword 3

Executive Summary 11

Welcome 15

D-S. Yoon
Congratulatory Address 17

I-S. Chang
Welcome Address 19

G.H. Marcus
OECD Welcome 21

GENERAL SESSION: ACCELERATOR PROGRAMMES AND APPLICATIONS 23

CHAIRS: B-H. CHOI, R. SHEFFIELD

T. Mukaiyama
Background/Perspective 25

M. Salvatores
Accelerator-driven Systems in Advanced Fuel Cycles 27

S. Noguchi
Present Status of the J-PARC Accelerator Complex 37

H. Takano
R&D of ADS in Japan 45

R.W. Garnett, A.J. Jason
Los Alamos Perspective on High-intensity Accelerators 57

J-M. Lagniel
French Accelerator Research for ADS Developments 69

T-Y. Song, J-E. Cha, C-H. Cho, C-H. Cho, Y. Kim, B-O. Lee, B-S. Lee, W-S. Park, M-J. Shin
Hybrid Power Extraction Reactor (HYPER) Project 81

V.P. Bhatnagar, S. Casalta, M. Hugon
Research and Development on Accelerator-driven Systems in the EURATOM 5th and 6th Framework Programmes 89

S. Monti, L. Picardi, C. Rubbia, M. Salvatores, F. Troiani
Status of the TRADE Experiment 101

P. D'hondt, B. Carluec
The European Project PDS-XADS "Preliminary Design Studies of an Experimental Accelerator-driven System" 113

F. Groeschel, A. Cadiou, C. Fazio, T. Kirchner, G. Laffont, K. Thomsen
Status of the MEGAPIE Project 125

P. Pierini, L. Burgazzi
ADS Accelerator Reliability Activities in Europe 137

W. Gudowski
ADS Neutronics 149

P. Coddington
ADS Safety 151

Y. Cho
Technological Aspects and Challenges for High-power Proton Accelerator-driven System Application 153

TECHNICAL SESSION I: ACCELERATOR RELIABILITY 163

CHAIRS: A. MUELLER, P. PIERINI

D. Vandeplassche, Y. Jongen (for the PDS-XADS Working Package 3 Collaboration)
The PDS-XADS Reference Accelerator 165

N. Ouchi, N. Akaoka, H. Asano, E. Chishiro, Y. Namekawa, H. Suzuki, T. Ueno, S. Noguchi, E. Kako, N. Ohuchi, K. Saito, T. Shishido, K. Tsuchiya, K. Ohkubo, M. Matsuoka, K. Sennyu, T. Murai, T. Ohtani, C. Tsukishima
Development of a Superconducting Proton Linac for ADS 175

C. Miélot
Spoke Cavities: An Asset for the High Reliability of a Superconducting Accelerator; Studies and Test Results of a $\beta = 0.35$, Two-gap Prototype and its Power Coupler at IPN Orsay 185

X.L. Guan, S.N. Fu, B.C. Cui, H.F. Ouyang, Z.H. Zhang, W.W. Xu, T.G. Xu
Chinese Status of HPPA Development 195

J.L. Biarrotte, M. Novati, P. Pierini, H. Safa, D. Uriot
Beam Dynamics Studies for the Fault Tolerance Assessment
of the PDS-XADS Linac 203

P.A. Schmelzbach
High-energy Beat Transport Lines and Delivery System
for Intense Proton Beams 215

M. Tanigaki, K. Mishima, S. Shiroya, Y. Ishi,
S. Fukumoto, S. Machida, Y. Mori, M. Inoue
Construction of a FFAG Complex for ADS Research in KURRI 217

G. Ciavola, L. Celona, S. Gammino, L. Andò, M. Presti,
A. Galatà, F. Chines, S. Passarello, XZh. Zhang, M. Winkler,
R. Gobin, R. Ferdinand, J. Sherman
Improvement of Reliability of the TRASCO
Intense Proton Source (TRIPS) at INFN-LNS 223

R.W. Garnett, F.L. Krawczyk, G.H. Neuschaefer
An Improved Superconducting ADS Driver Linac Design..... 235

A.P. Durkin, I.V. Shumakov, S.V. Vinogradov
Methods and Codes for Estimation of Tolerance
in Reliable Radiation-free High-power Linac 245

S. Henderson
Status of the Spallation Neutron Source Accelerator Complex 257

TECHNICAL SESSION II: TARGET, WINDOW AND COOLANT TECHNOLOGY..... 265

CHAIRS: X. CHENG, T-Y. SONG

Y. Kurata, K. Kikuchi, S. Saito, K. Kamata, T. Kitano, H. Oigawa
Research and Development on Lead-bismuth Technology
for Accelerator-driven Transmutation System at JAERI 267

P. Michelato, E. Bari, E. Cavaliere, L. Monaco, D. Sertore,
A. Bonucci, R. Giannantonio, L. Cinotti, P. Turroni
Vacuum Gas Dynamics Investigation and Experimental Results
on the TRASCO ADS Windowless Interface 279

J-E. Cha, C-H. Cho, T-Y. Song
Corrosion Tests in the Static Condition and Installation
of Corrosion Loop at KAERI for Lead-bismuth Eutectic 291

P. Schuurmans, P. Kupschus, A. Verstrepen, J. Cools, H. Aït Abderrahim
The Vacuum Interface Compatibility Experiment (VICE)
Supporting the MYRRHA Windowless Target Design 301

C-H. Cho, Y. Kim, T-Y. Song
Introduction of a Dual Injection Tube for the Design
of a 20 MW Lead-bismuth Target System 313

H. Oigawa, K. Tsujimoto, K. Kikuchi, Y. Kurata, T. Sasa, M. Umeno, K. Nishihara, S. Saito, M. Mizumoto, H. Takano, K. Nakai, A. Iwata
Design Study Around Beam Window of ADS 325

S. Fan, W. Luo, F. Yan, H. Zhang, Z. Zhao
Primary Isotopic Yields for MSDM Calculations of Spallation
Reactions on ^{280}Pb with Proton Energy of 1 GeV 335

N. Tak, H-J. Neitzel, X. Cheng
CFD Analysis on the Active Part of Window Target Unit
for LBE-cooled XADS 343

T. Sawada, M. Orito, H. Kobayashi, T. Sasa, V. Artisyuk
Optimisation of a Code to Improve Spallation Yield Predictions
in an ADS Target System 355

TECHNICAL SESSION III: SUBCRITICAL SYSTEM DESIGN AND ADS SIMULATIONS 363

CHAIRS: W. GUDOWSKI, H. OIGAWA

T. Misawa, H. Unesaki, C.H. Pyeon, C. Ichihara, S. Shiroya
Research on the Accelerator-driven Subcritical Reactor at the Kyoto
University Critical Assembly (KUCA) with an FFAG Proton Accelerator 365

K. Nishihara, K. Tsujimoto, H. Oigawa
Improvement of Burn-up Swing for an Accelerator-driven System 373

S. Monti, L. Picardi, C. Ronsivalle, C. Rubbia, F. Troiani
Status of the Conceptual Design of an Accelerator
and Beam Transport Line for Trade 383

A.M. Degtyarev, A.K. Kalugin, L.I. Ponomarev
Estimation of some Characteristics of the
Cascade Subcritical Molten Salt Reactor (CSMSR) 393

F. Roelofs, E. Komen, K. Van Tichelen, P. Kupschus, H. Aït Abderrahim
CFD Analysis of the Heavy Liquid Metal Flow Field
in the MYRRHA Pool 401

A. D'Angelo, B. Arien, V. Sobolev, G. Van den Eynde, H. Aït Abderrahim, F. Gabrielli
Results of the Second Phase of Calculations Relevant to
the WPPT Benchmark on Beam Interruptions 411

TECHNICAL SESSION IV: SAFETY AND CONTROL OF ADS 423

CHAIRS: J-M. LAGNIEL, P. CODDINGTON

P. Coddington, K. Mikityuk, M. Schikorr, W. Maschek, R. Sehgal, J. Champigny, L. Mansani, P. Meloni, H. Wider
Safety Analysis of the EU PDS-XADS Designs 425

X-N. Chen, T. Suzuki, A. Rineiski, C. Matzerath-Boccaccini, E. Wiegner, W. Maschek
Comparative Transient Analyses of Accelerator-driven Systems with Mixed Oxide and Advanced Fertile-free Fuels 439

P. Coddington, K. Mikityuk, R. Chawla
Comparative Transient Analysis of Pb/Bi and Gas-cooled XADS Concepts 453

B.R. Sehgal, W.M. Ma, A. Karbojian
Thermal-hydraulic Experiments on the TALL LBE Test Facility 465

K. Nishihara, H. Oigawa
Analysis of Lead-bismuth Eutectic Flowing into Beam Duct 477

P.M. Bokov, D. Ridikas, I.S. Slessarev
On the Supplementary Feedback Effect Specific for Accelerator-coupled Systems (ACS) 485

W. Haeck, H. Aït Abderrahim, C. Wagemans
K_{eff} and K_s Burn-up Swing Compensation in MYRRHA 495

TECHNICAL SESSION V: ADS EXPERIMENTS AND TEST FACILITIES 505

CHAIRS: P. D'HONDT, V. BHATNAGAR

H. Oigawa, T. Sasa, K. Kikuchi, K. Nishihara, Y. Kurata, M. Umeno, K. Tsujimoto, S. Saito, M. Futakawa, M. Mizumoto, H. Takano
Concept of Transmutation Experimental Facility 507

M. Hron, M. Mikisek, I. Peka, P. Hosnedl
Experimental Verification of Selected Transmutation Technology and Materials for Basic Components of a Demonstration Transmuter with Liquid Fuel Based on Molten Fluorides (Development of New Technologies for Nuclear Incineration of PWR Spent Fuel in the Czech Republic) 519

Y. Kim, T-Y. Song
Application of the HYPER System to the DUPIC Fuel Cycle 529

M. Plaschy, S. Pelloni, P. Coddington, R. Chawla, G. Rimpault, F. Mellier
Numerical Comparisons Between Neutronic Characteristics of MUSE4 Configurations and XADS-type Models 539

B-S. Lee, Y. Kim, J-H. Lee, T-Y. Song
Thermal Stability of the U-Zr Fuel and its Interfacial Reaction with Lead 549

SUMMARIES OF TECHNICAL SESSIONS 557

CHAIRS: R. SHEFFIELD, B-H. CHOI

Chairs: A.C. Mueller, P. Pierini
Summary of Technical Session I: Accelerator Reliability 559

Chairs: X. Cheng, T-Y. Song
Summary of Technical Session II: Target, Window
and Coolant Technology 565

Chairs: W. Gudowski, H. Oigawa
Summary of Technical Session III: Subcritical System Design
and ADS Simulations 571

Chairs: J-M. Lagniel, P. Coddington
Summary of Technical Session IV: Safety and Control of ADS 575

Chairs: P. D'hondt, V. Bhatagnar
Summary of Technical Session V: ADS Experiments and Test Facilities 577

SUMMARIES OF WORKING GROUP DISCUSSION SESSIONS 581

CHAIRS: R. SHEFFIELD, B-H. CHOI

Chair: P.K. Sigg
Summary of Working Group Discussion on Accelerators 583

Chair: W. Gudowski
Summary of Working Group Discussion on Subcritical Systems
and Interface Engineering 587

Chair: P. Coddington
Summary of Working Group Discussion on Safety and Control of ADS 591

Annex 1: List of workshop organisers 595

Annex 2: List of participants 597

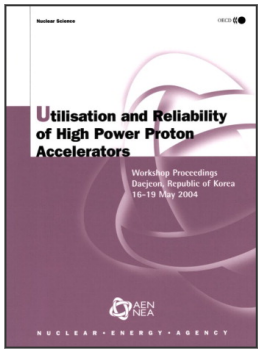

From:

Utilisation and Reliability of High Power Proton Accelerators

Workshop Proceedings, Daejeon, Republic of Korea, 16-19 May 2004

Access the complete publication at:

https://doi.org/10.1787/9789264013810-en

Please cite this chapter as:

Ouchi, Nobuo, *et al.* (2006), "Development of a Superconducting Proton Linac for ADS", in OECD/Nuclear Energy Agency, *Utilisation and Reliability of High Power Proton Accelerators: Workshop Proceedings, Daejeon, Republic of Korea, 16-19 May 2004*, OECD Publishing, Paris.

DOI: https://doi.org/10.1787/9789264013810-19-en

This work is published under the responsibility of the Secretary-General of the OECD. The opinions expressed and arguments employed herein do not necessarily reflect the official views of OECD member countries.

This document and any map included herein are without prejudice to the status of or sovereignty over any territory, to the delimitation of international frontiers and boundaries and to the name of any territory, city or area.

You can copy, download or print OECD content for your own use, and you can include excerpts from OECD publications, databases and multimedia products in your own documents, presentations, blogs, websites and teaching materials, provided that suitable acknowledgment of OECD as source and copyright owner is given. All requests for public or commercial use and translation rights should be submitted to rights@oecd.org. Requests for permission to photocopy portions of this material for public or commercial use shall be addressed directly to the Copyright Clearance Center (CCC) at info@copyright.com or the Centre français d'exploitation du droit de copie (CFC) at contact@cfcopies.com.